

6 Due Date

7 Abstract

8 How does the brain process and represent successive sound in close temporal proximity? By
9 investigating mismatch negativity (MMN) components, prior research (Sussman & Gumenyuk,
10 2005; Sussman, Ritter & Vaughan, 1998) has suggested that temporal proximity plays an
11 important role in how sounds are represented in auditory memory. Here, we investigate how
12 predictability affects the election of mismatch negativity components in auditory sequences
13 consisting of two tones (frequent tone A = 440 Hz, rare tone B = 494 Hz, fixed SOA 100 ms). In
14 the predictable condition, tones are presented in a fixed order whereas in the unpredictable
15 condition, standards and deviants are presented in a pseudo-random order. We expect to find
16 that B tones in the unpredictable condition will elicit a significant MMN while B tones in the
17 predictable conditions will not. A repeating five-tone pattern was presented at several stimulus
18 rates (200, 400, 600, and 800 ms onset-to-onset) to determine at what temporal proximity the
19 five-tone repeating unit would be represented in memory. The mismatch negativity component
20 of event-related brain potentials was used to index how the sounds were organized in memory
21 when participants had no task with the sounds. Only at the 200-ms onset-to-onset pace was the
22 five-tone sequence unitized in memory. At presentation rates of 400 ms and above, the regularity
23 (a different frequency tone occurred every fifth tone) was not detected and mismatch negativity
24 was elicited by these tones in the sequence. The results show that temporal proximity plays a role
25 in unitizing successive sounds in auditory memory. These results also suggest that global
26 relationships between successive sounds are represented at the level of auditory cortices.

27	Revisiting the Stimulation-Rate-Dependent Pattern	
28	Mismatch Negativity	
29		
30	Abstract	2
31	Revisiting the Stimulation-Rate-Dependent Pattern Mismatch Negativity	3
32	Introduction	4
33	Design and Hypotheses	7
34	Methods and Materials	10
35	Data Acquisition	10
36	Participants	10
37	Stimuli and Stimulus Delivery	10
38	Data Acquisition	12
39	Analysis Pipeline	12
40	Statistical Analysis	13
41	Results	16
42	Discussion	24

Introduction

Unraveling the mysteries of human perception might be one of the most fascinating and difficult challenges in cognitive sciences. Mostly unnoticed and at every moment in our lives, we achieve something outstanding: By forming a coherent representation from the tangled mess of external stimuli that reach our senses, we make sense of the outside world. Seemingly effortlessly, in doing so we solve complicated mathematical problems such as the inverse problem. Recent advances in fields like computer vision and machine hearing have provided a sense of how daunting these tasks can be - requiring complex models consuming vast amounts of computational resources and energy. What enables the brain to fulfill these functions with such ease while consuming no more than a lightbulb's power equivalent?

Over the centuries, many theories have been brought forward attempting to answer these questions. Great philosophers like Plato, Kant and Locke had varying success in developing their own ideas on the inner workings of perception. Among the first who developed a consistent theory of the rules that perception follows, were the Gestalt psychologists of the early 20th century. Wertheimer, Koffka, and Köhler hypothesized that so-called Gestalt principles, rules on how individual elements should be grouped or separated, would guide perception. Their concept was based on the observation that humans tend to perceive integrated patterns as opposed to just collection of individual elements.

Much later, auditory scientists faced the same challenge described earlier, but now in a very specific context. They were puzzled: How does the brain form meaningful perceptual experiences from what can only be described as a busy mess of sound waves that originate from a myriad of different sources differing in pitch, loudness, and spatial position. Known as the *cocktail party effect*, this problem is often compared to inferring the positions, shapes and movements of boats on a lake - just by observing how two nearby objects move up and down on the waves. Attempts to find answers to this perplexing question lead to the development of auditory scene analysis (ASA). Not unlike the concepts proposed by the Gestalt theorists some decades earlier, (Bregman?) suggested that the brain uses so-called *streaming* and *segregation* to form auditory objects from rich spectro-temporal information. Auditory scene analysis relies on two different

categories of grouping, called sequential and simultaneous integration. Simultaneous or vertical integration refers to the grouping of concurrent properties into one or more separable auditory objects, a process informed by temporal cues like common onset and offset, spectral and spatial characteristics among others. Sequential integration on the other hand describes how temporally distinct sounds are merged into one or multiple coherently perceived stream (contrary to simultaneous grouping, only one such stream can be actively perceived at any time). While vertical and horizontal grouping can come to different and therefore competing results (**needsref?**), sequential grouping often takes precedence over cues for simultaneous integration (**needsref?**),

As is so often the case, the key to understanding such complex phenomena seems to lie in learning about the most basic processing steps. In auditory research this steps usually come in the shape of simple stimuli, often consisting of nothing more than pure tones. The auditory oddball paradigm is a well-established and robust paradigm extensively used in event related potential (ERP) studies. In its basic form, participants are presented with a series of similar tones or sounds (so-called *standard* events), interrupted by rare tones or sounds that differ in at least one feature (*deviant* events) from the more frequent ones. Strikingly, deviant events elicit larger neural activity over sensory areas - a finding that is known as the mismatch negativity (MMN) component, because when measured using EEG, a robust negative deflection can be observed obtained by subtracting the response to deviant events from the response to standard events. Negativity is strongest in the fronto-temporal area of the scalp with a peak latency ranging from 100 to 250 ms after stimulus onset. The elicition of MMN is not restricted to the repetition of physically identical stimuli but can also be observed when deviant events are of complex nature, e.g. when abstract auditory regularities are violated (Paavilainen, 2013). The regularities can come in the form of relationships between two (Saarinen et al., 1992) or multiple tones (Alain et al., 1994; Nordby et al., 1988; Schröger et al., 1996). Interestingly, this finding is also highly compatible with another prevalent theory of perception: The idea that prediction informs how humans perceive the world. These kind of ideas have been around a long time and famously trace back to the remarkable physiologist Hermann von Helmholtz. In its most recent iteration, this theory has been known as (hierarchical) predictive coding. These theories vary in how much relative weight they assign to bottom-up processing and prediction. But regardless of how one might

interpret this relation, the observation of MMN almost inevitably leads to an interpretation in which the processing of deviant signals can be regarded as a violation of expectation. As such, these error signals play an important role in understanding prediction, expectation and perception in the human brain.

But how does the brain handle situations in which concurrent but contradictory predictive clues exist? Following this idea, E. Sussman et al. (1998) presented participants with a sequence of frequent pure tones and rare pitch deviants while reading a book of their choice. Tones were arranged in a predictable five-tone pattern consisting of four standard tones and one deviant (i.e. A-A-A-A-B-A-A-A-B, "-" indicating silence between the tones). ERPs to A and B tones were compared for rapid (SOA of 100 ms) and slow (SOA of 1200 ms) stimulation rates. For the 100 ms SOA, they also included a control condition in which tone order was pseudo-random (e.g. A-A-A-B-A-B-A-A-A) without altering deviant probability ($p_B = 20\%$). When tones are presented randomly, only their relative frequency of occurrence carries value for predicting the pitch of the next tone. This, we refer to as *proportional regularity*. In an ordered presentation however, a sequence of four standard tones is always followed by a deviant tone. Thus, understanding this relationship should allow for *perfect* precision in which all deviant tones are expected with near-absolute certainty. We call this regularity a *pattern regularity*. Provided the underlying mechanism can incorporate such information, the processing of the pitch deviants should correspond with that of standard tones and therefore no MMN would be elicited. Interestingly, in the case of Sussman et al., MMNs were only elicited if tone presentation was slow and predictable or fast and random, but not when predictable tones were presented in a rapid fashion. In a subsequent study, E. S. Sussman & Gumenyuk (2005) used the same pattern at different SOAs (200 ms, 400 ms, and 800 ms). Similarly to their previous study, ordered presentation at 400 ms and 800 ms SOA elicited an MMN response, while at a stimulation rate of 200 ms evidence for such a deflection was absent. Sussman et al. attributed this observation to sensory memory limitations. That is, only when auditory memory can accommodate enough repetitions of the five-tone pattern, tones could be integrated into a coherent representation allowing for accurate predictions of deviant tones. This, in turn, would explain the absence of MMNs in the fast presentation condition. Based on this, they argued that while true for fast

presentation rates with SOAs up to 200 ms, for longer SOAs pattern durations would be too long and thus representations would exceed sensory memory capacity.

In a recent in-class replication study, Scharf & Müller (in prep) presented participants with the same stimuli as Sussmann in a very similar experimental setting. Their study only differed in that participants were given a simple task in which they had to count visual targets instead of reading a book of their choice. Surprisingly, while descriptive results were compatible with those of Sussmann et al., pairwise comparison revealed no significant effect when comparing deviant and standard tones for both the *random* and the *predictable* condition. Further Bayesian analysis remained largely inconclusive, providing only *anecdotal* evidence in favor of such an effect for *random* presentation and *moderate* evidence for its absence in the *predictable* condition. In the face of the replication crisis, many scientists have become painfully aware of the importance of replicability. It is clear that exact or quasi-exact replication studies that try to match experimental conditions of the original study as closely as possible are one key to more reliable research results (Popper, 1935). However, replications that extend, change or optimize materials or methods of the original work also offer valuable insight. These forms of replications are known as conceptual (Schmidt, 2009) and refer to the use of different methods to repeat the test of a hypothesis or experimental result.

Design and Hypotheses

In this thesis, we try to answer the very same question Sussman et al. posed: When first-order as well as higher-order relationships between auditory events can offer concurrent but varying degrees of predictive value, what information is used? We largely follow the procedure laid out by E. S. Sussman & Gumenyuk (2005) though we deviate in some important aspects. First, aforementioned five-tone patterns are not only presented in the *predictable* condition, but also in the *random* context. That is, pseudo-random order will be deliberately broken by occasionally presenting B-A-A-A-A-B-patterns. In particular, this will make sure that the local history of B-tones in the *random* condition is comparable to that in the *predictable* condition. Secondly, B tones are compared exclusively with their preceding A tones. And lastly, a small number of

A-A-A-A-B will be replaced by A-A-A-A-A sequences. The expected advantages of this design are discussed in more detail in the hypothesis section. A pre-registration covering data collection, processing, and analysis is available at <https://osf.io/cg2zd/>. Deviations from this pre-specified plan and further, exploratory analysis will be clearly marked.

E. S. Sussman & Gumenyuk (2005) interpretation of the original results would suggest that at fast stimulation rates, pattern-based regularities take precedence over proportion-based regularities. If this is indeed the case, B-tones in the *predictable* condition should not be considered a *mismatch* and thus should not elicit an MMN. In contrast, since there is no way to reliably predict B-tones in the *random* condition, these tones would be still considered as *deviant* events and are therefore expected to generate a MMN.

Specifically, the hypotheses are concerned with the ERPs elicited by the 5th tone in the five-tone sequence (A-A-A-A-B or A-A-A-A-A) compared to the 4th tone in that sequence (A-A-A-A-X, “X” marking either an A or an B tone).

We will also compare the respective difference waves (A-A-A-A-B vs. A-A-A-A-B) in the *predictable* condition with that in the *random* condition.

In summary, i) one expects negativity in the N1/MMN time domain (about 100-200 ms after the beginning of the tone) for deviations in the BAAAAB sequence in the *random* condition, since B tones violate the *proportional regularity*, ii) one expects no evidence for such an effect (or evidence favoring \mathcal{H}_0 i.e. that there is no effect) in the *predictable* context since more informative higher-order predictions based on *pattern regularity* are not violated, and iii) the difference waves should differ significantly. If however no *pattern regularity* is extracted, B-tones should consistently elicit an MMN regardless of presentation context since the predictive value of the *proportional regularity* does not differ between conditions. In that case, difference waves should not differ. As a third possibility, the brain might use *proportional regularities* and *pattern regularities* concurrently, resulting in a negativity following B-tones in either condition. To further differentiate between these explanations, we also expect the comparison of 5th A tones to preceding A tones (A-A-A-A-X vs. A-A-A-A-A) to elicit a significant MMN for options i and iii,

¹⁸³ but not for option ii.

Methods and Materials

Data Acquisition

Participants

100 ms Presentation Rate Twenty-three psychology undergraduate students (2 males, average age 22.6 yrs., $SD = 5.57$, range 18 - 42 yrs.) were recruited at the Institute of Psychology at the University of Leipzig. All participants reported good general health, normal hearing and had normal or corrected-to-normal vision. Written informed consent was obtained before the experiment. One-third (34.8%) of participants spent time enaging in musical activities at time of survey, while 8.7% had no prior experience in music training. Handedness was asseced using a modified version of the Edinburgh Handedness Inventory (Oldfield, 1971, see appendix). A majoritiy (00%) of parcipiants favored the right hand. Participants were blinded in respect to the purpose of the experiment and received course credit in compensation.

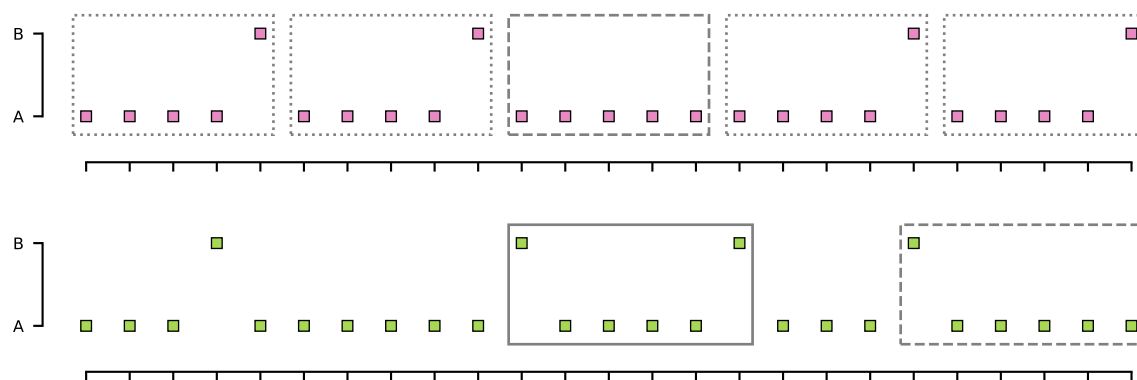
150 ms Presentation Rate Twenty healthy participants (0 males, average age 00.0 yrs., $SD = 0.00$, range 00 - 00 yrs.) were recruited. Participants gave informed consent and reported normal hearing and corrected or corrected-to-normal vision. All participants were naive regarding the purpose of the experiment and were compensated in course credit or money. 00 participants (00%) had received musical training in the last 5 years before the experiment while 00 (00%) reported no musical experiance. In addition, participants reported if streaming occured during the presentation of the tones.

Stimuli and Stimulus Delivery

Participants where seated in a comfortable chair in a sound-insulated cabin. The experimental setup was practically the same as the one used ny Sussman, but instead of reading a book, subjects were asked to focus their attention on a previously selected movie. Movies were presented with subtitles but without sound. Commercially available software (MATLAB R2014a; The MathWorks Inc, Natick, MA) in conjunction with the Psychophysics Toolbox extension (version 3.0.12, Brainard, 1997; Kleiner et al., 2007) was used to control stimulus presentation.

Figure 1.

Tones of two different frequencies ($A=440$ Hz, $B=449$ Hz) were presented in two blocked conditions: In the “predictable” condition (top half), tones followed a simple pattern in which a single B-tone followed four A-tones. Some designated B-tones were replaced by A-tones (“pattern deviants”). In the “random” condition (lower half), tones were presented in a pseudo-random fashion ()



Stimuli consisted of pure sinusoidal tones with a duration of 50 ms (including a 10 ms cosine on/off ramp), presented isochronously at a stimulation onsets asynchrony (SOA) of 100 ms for study 1 and 150 ms for study 2. Overall, a total of 40 blocks containing a mixture of frequent 440 Hz tones (“A” tones) and infrequent 449 Hz tones (“B” tones) were delivered binaurally using Sennheiser HD-25-1 II headphones. In one half of the blocks, tones were presented in pseudo-random order (e.g. A-A-A-B-A-B-A), “random” condition), while in the remaining block tone presentation followed a simple pattern in which a five-tone-sequence of four frequent tones and one infrequent tone (i.e. A-A-A-A-B) was repeated cyclically (“predictable” condition). Block order was counterbalanced accross participants. The ratio of frequent and infrequent tones was 10% for both conditions. Within the predictable condition, 10% of designated (infrequent) B tones were replaced by A tones, resulting in sporadic five-tone sequences consisting solely of A tones (i.e. A-A-A-A-A), thus violating the predictability rule. To assure comparability of local histories between tones in both conditions, randomly arranged tones were interspersed with sequences mimicking aforementioned patterns from the predictable condition (B-A-A-A-A-B and B-A-A-A-A-A) in the random condition. A grand total of 2000 tones in study 1 and 4000 tones in study 2 were delivered to each participant.

Data Acquisition

Electrophysiological data was recorded from active silver-silver-chloride (Ag-AgCl) electrodes using an ActiveTwo amplifier system (BioSemi B.V., Amsterdam, The Netherlands). Acquisition was monitored online to ensure optimal data quality. A total of 39 channels were obtained using a 32-electrode-cap and 7 external electrodes. Scalp electrode locations conformed to the international 10–20 system. Horizontal and vertical eye movement was obtained using two bipolar configurations with electrodes placed around the lateral canthi of the eyes and above and below the right eye. Additionally, electrodes were placed on the tip of the nose and at the left and right mastoid sites. Data was sampled at 512 Hz and on-line filtered at 1000 Hz.

Analysis Pipeline

Data preprocessing was implemented using a custom pipeline based on the *MNE Python* software package (Gramfort, 2013) using *Python 3.7*. All computations were carried out on a cluster operated by the University Computation Center of the University of Leipzig. Code used in thesis is publicly available at <https://github.com/marcpabst/xmas-oddballmatch>.

First, EEG data was subjected to the ZapLine procedure (de Cheveigné, 2020) to remove line noise contamination. A fivefold detection procedure as described by Bigdely-Shamlo et al. (2015) was then used to detect and subsequently interpolate bad channels. This specifically included the detection of channels that contain prolonged segments with very small values (i.e. flat channels), the exclusion of channels based on robust standard deviation (deviation criterion), unusually pronounced high-frequency noise (noisiness criterion), and the removal of channels that were poorly predicted by nearby channels (correlation criterion and predictability criterion). Channels considered bad by one or more of these methods were removed and interpolated using spherical splines (Perrin et al., 1989). Electrode locations for interpolations were informed by the BESA Spherical Head Model.

For independent component analysis (ICA), a 1-Hz-high-pass filter (134th order hamming-windowed FIR) was applied prior to ICA (Winkler et al., 2015). To further reduce artifacts, Artifact Subspace Reconstruction (ASR, Mullen et al., 2015) was used to identify and

remove parts of the data with unusual characteristics (bursts). ICA was then carried out using the *Picard* algorithm (Ablin et al., 2018, 2017) on PCA-whitened data. To avoid rank-deficiency when extracting components from data with one or more interpolated channels, PCA was also used for dimensionality reduction. The EEGLAB (version 2020.0, Delorme & Makeig, 2004) software package and the IClable plugin (version 1.2.6, Pion-Tonachini et al., 2019) were used to automatically classify estimated components. Only components clearly classified (i.e. confidence above 50%) as resulting from either eye movement, muscular, or heartbeat activity were zeroed-out before applying the mixing matrix to unfiltered data.

In line with recommendations from Widmann et al. (2015) and de Cheveigné & Nelken (2019), a ORDER finite impulse response (FIR) bandpass filter from 0.1 Hz to 40 Hz (Hamming window, 0.1 Hz lower bandwidth, 4 Hz upper bandwidth, 0.0194 passband ripple, and 53 dB stopband attenuation). Continuous data was epoched into 400 ms long segments around stimulus onsets. Epochs included a 100 ms pre-stimulus interval. No baseline correction was applied. Segments exceeding a peak-to-peak voltage difference of 100 μ V were removed. On average, NN epochs No data set meet the pre-registered exclusion criterion stated of less than 100 trials per condition, thus data from all participants (20 for 100 ms presentation rate and 23 for 150 ms presentation rate) was analysed.

Statistical Analysis

Statistical Analysis was carried out using the R programming language (version 3.2). Dependent variables quantifying mismatch negativity response were calculated by averaging amplitudes in a time window stretching ± 25 ms around the maximum negativity obtained by subtracting the mean ERP timecourse following the A tones from the mean ERP following B tones. To compute mean amplitudes, ERPs to 4th position A tones (A-A-A-A-X, **boldface** indicates the tone of interest) and B tones (A-A-A-A-B) were averaged separately for both the *random* and the *predictable condition*. For the *random condition*, only tones that were part of a sequence matching the patterns in the *predictable* condition were included.

In accordance with the original analysis by E. S. Sussman & Gumenyuk (2005), mean

amplitudes for frontocentral electrodes (FZ, F3, F4, FC1, and FC2) and the two mastoid positions (M1 and M2) were averaged separately. Then, for both SOAs, independent three-way repeated measures analyses of variance with factors *condition* (factors *predictable* and *random*), *stimulus type* (factors *A tone* and *B tone*), *electrode locations* (levels *fronto-central* and *mastoids*), and all possible interactions were calculated. Following this, significant interaction effects were further investigated using post-hoc *t*-tests.

Besides the fact that p-values are frequently misinterpreted (Hubbard, 2011), traditional null hypothesis testing fails to explicitly quantify evidence in favor of \mathcal{H}_0 (e.g. Aczel et al., 2018; Goodman, 2008; Kirk, 1996; Meehl, 1978). Similarly, p-values can exaggerate evidence against \mathcal{H}_0 (that is, observed data might be more likely under \mathcal{H}_0 than under \mathcal{H}_1 even though \mathcal{H}_0 is rejected e.g., Hubbard & Lindsay, 2008; Rouder et al., 2009; Sellke et al., 2001; Wagenmakers et al., 2018).¹ Conversely, Bayesian hypothesis testing using Bayes factors can provide an intuitive way to compare observed data's likelihood under the null hypothesis versus the alternative hypothesis (Wagenmakers, 2007): $BF_{10} = \frac{Pr(data|\mathcal{H}_0)}{Pr(data|\mathcal{H}_1)}$. Here, this approach was applied in agreement with the concept described by Rouder et al. (2009) as an alternative to classical frequentist paired *t*-tests. Following this notion, Bayes factors for within-participant differences y_i were computed assuming $\mathcal{H}_0 : y_i \sim Normal(0, \sigma^2)$ and $\mathcal{H}_1 : y_i \sim Normal(\delta, \sigma^2); \delta \sim Cauchy(0, 1/\sqrt{2})$. A Jeffreys prior was used for the variance σ^2 in both models: $p(\sigma^2) \propto 1/\sigma^2$. Calculations were performed using the Hamiltonian Monte Carlo method implemented in *Stan* (version 2.25, Carpenter et al., 2017) and *RStan* (Stan Development Team, 2020).

Finally, the relationship between epoch number and the reliability analysis was analyzed by drawing random subsamples of different sizes from both our data sets and calculating split-half reliability employing the Spearman-Brown approach. For this, single trial responses for all A and B tones in the predictable condition were randomly shuffled. Then, 100, 200, ..., N_{max} ($N_{max,100ms} = 3000, N_{max,150ms} = 1500$) epochs were drawn, randomly assigned to one of two halves, and afterwards averaged separately for both tone types. Then, split-half reliability was calculated using the differences between A and B tones in the MMN

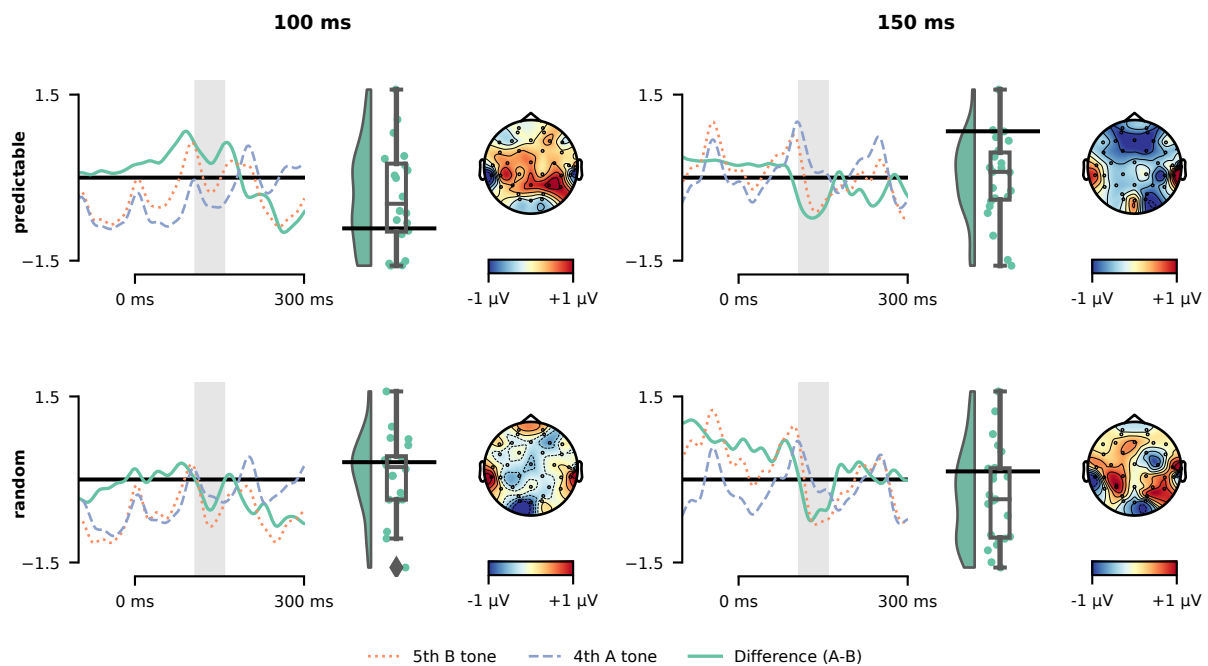
¹ it doesn't quantify evidence in favor of the \mathcal{H}_1 , either

307 latency window using the Sprearman-Brown prophecy formula² (Brown, 1910; Spearman, 1910).
308 This procedure was repeated 100 times for each N and split-half-relaibilites thus obtained were
309 subsequently averaged.

² as given by $\rho_{xx'} = \frac{2\rho_{12}}{1+\rho_{12}}$, where ρ_{12} is the Pearson correlation coefficient between the two halves.

Figure 2.

ERP grand averages (pooled FZ, F3, F4, FC1, and FC2 electrode locations) for an SOA of 100 ms (left) and 150 ms (right), for A tones (A-A-A-A-X, blue dashed lines) and B tones (A-A-A-A-B, orange dashed line) and their difference (B - A, green solid line). Upper panels show ERPs for tones presented in a predictable pattern (predictable condition) while lower panels show ERPs for tones presented in pseudo-random order (random condition). Shaded area marks MMN latency window (110 ms to 160 ms) used to calculate the distribution of amplitude differences across participants (middle of each panel) and the difference of topographic maps averaged over the same interval (right of each panel).

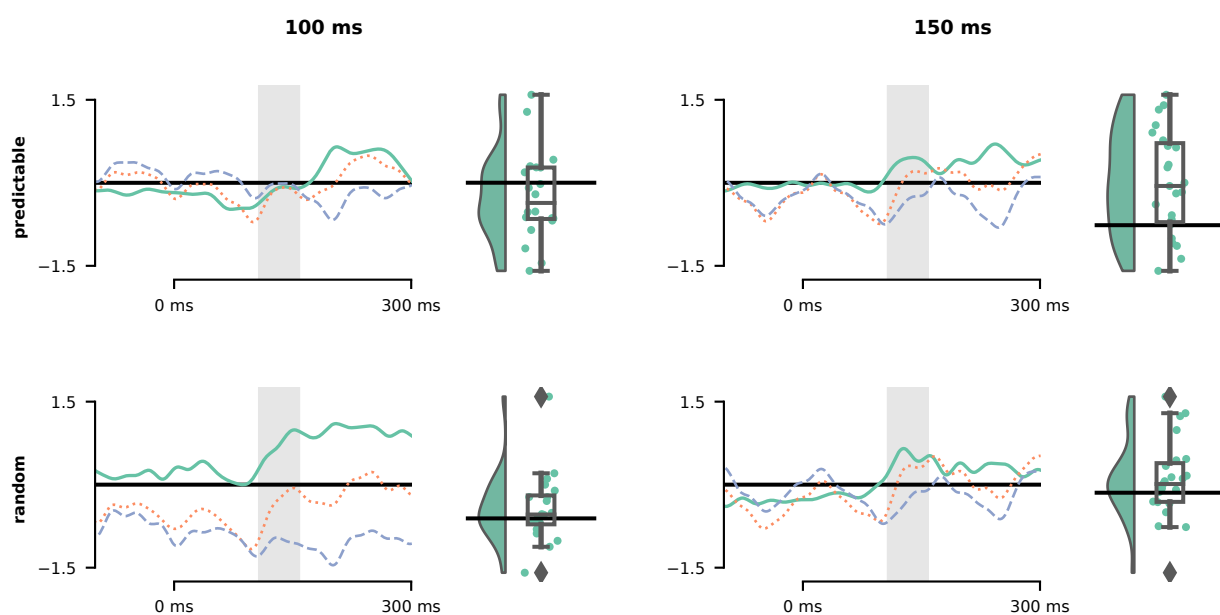


Results

Grand averages of event-related potentials (ERP) at pooled FZ, F3, F4, FC1, and FC2 electrode locations to A tones (A-A-A-A-X), B tones (A-A-A-A-B), and their difference (B tone minus A tone) are displayed in fig. 2 for both 100 ms (left panel) and 150 ms (right panel) stimulus onset asynchronies. The top half of each panel shows ERPs in the *predictable condition* while the lower half depicts ERPs in the *random condition*. For both presentation rates, clear rhythms matching the presentation frequency of 10 Hz (100 ms) and respectively 6.667 Hz (150 ms) are seen as a result of substantial overlap of neighbouring tones. Panels also show the distribution of mean amplitude differences in the MMN latency window (as defined above, 110 ms to 160 ms after

Figure 3.

ERP grand averages (pooled M1, M2 electrode locations) for an SOA of 100 ms (left) and 150 ms (right), for A tones (A-A-A-A-X, blue dashed lines) and B tones (A-A-A-A-B, orange dashed line) and their difference (B - A, green solid line). Upper panels show ERPs for tones presented in a predictable pattern (predictable condition) while lower panels show ERPs for tones presented in pseudo-random order (random condition). Shaded area marks MMN latency window (110 ms to 160 ms) used to calculate the distribution of amplitude differences across participants.



stimulus onset) across participants and the difference of scalp topographies averaged over the same interval. Similarly, waveforms and mean amplitude difference distributions at pooled mastoid sites are shown in fig. 3.

Evoked responses to A and B tones were compared by calculating mean amplitudes in the MMN latency window. Mean amplitudes in the MMN latency window and their standard deviations (SD) for all conditions are shown in Table X. Descriptively, mean amplitudes at pooled fronto-central electrode locations were more negative for randomly presented B tones than for randomly presented A tones, regardless of tone presentation rate (100 ms: $\Delta M = -0.358 \mu V$; 150 ms: $\Delta M = -0.555 \mu V$) This also held for tones presented predictably, but for the slower of the two presentation rates only ($\Delta M = -0.582 \mu V$). In contrast, when predictable tone patterns occurred at a faster 100 ms rate, B tones elicited descriptively more positive responses than A

tones ($\Delta M = 0.383 \mu V$). Descriptive comparison of evoked responses from pooled left and right mastoids revealed that pseudo-randomly presented B tones were more positive in the MMN latency window than A tones (100-ms-SOA: $\Delta M = 0.746 \mu V$, 150-ms-SOA: $\Delta M = 0.510 \mu V$). A similar observation could be made for predictable B tones compared to the preceding A tones at an SOA of 150 ms ($\Delta M = 0.399 \mu V$) but not for the faster presentation rate ($\Delta M = -0.132 \mu V$).

Table 1

Means and standard deviations for condition, stimulus type and electrodes.

SOA	Condition	StimulusType	Mean	SD	Mean	SD
100	predictable	A	-0.431	1.23	-0.052	1.51
		B	-0.0477	1.22	-0.184	1.56
	random	A	-0.225	1.82	-1.04	2.64
		B	-0.583	2.16	-0.296	3.23
150	predictable	A	0.25	0.967	-0.349	1.19
		B	-0.331	1.09	0.0492	1.33
	random	A	0.0233	1.75	-0.292	1.64
		B	-0.531	1.82	0.218	2.38

Inference statistics provided support for these findings. For the 100 ms stimulation rate, the three-way ANOVA yielded a significant three-way interaction effect (*condition x stimulus type x electrode locations*; $F(1, 19) = 7.53, p = .013$) but failed to reveal main effects for factors *stimulus type* ($F(1, 19) = 1.05, p = .318$), *condition* ($F(1, 19) = 0.83, p = .373$), and *electrode locations* ($F(1, 19) = 0.04, p = .852$). In contrast, for tones presented at a SOA of 150 ms only the two-way interaction term *stimulus type x electrode locations* had a significant effect ($F(1, 22) = 20.76, p = 0.0002$). Mean amplitudes in the MMN latency window however did not differ for factors *stimulus type* ($F(1, 22) = 0.32, p = 0.5790$), *electrode locations* ($F(1, 22) = 0.04, p = 0.8540$) or *condition* ($F(1, 22) = 0.08, p = 0.7800$).

Two-way ANOVAs (*condition x stimulus type*) were carried out separately for pooled fronto-central and mastoid electrode locations. For 100 ms tone presentation rate, the *condition*

x *stimulus type* interaction only resulted in a significant effect for the fronto-central electrode cluster ($F(1, 19) = 16.75, p = 0.0006$) but not for pooled mastoid sites ($F(1, 19) = 2.37, p = 0.1410$) indicating that the three-way interaction effect *condition* x *stimulus type* x *electrode* is indeed driven by the amplitude differences in the fronto-central electrode locations. Contrary to this, for the 150 ms presentation rate, main effects for *stimulus type* were significant for both fronto-central and mastoid sites, suggesting that there was both an MMN at fronto-central locations as well as a polarity-reversal at the mastoid electrodes.

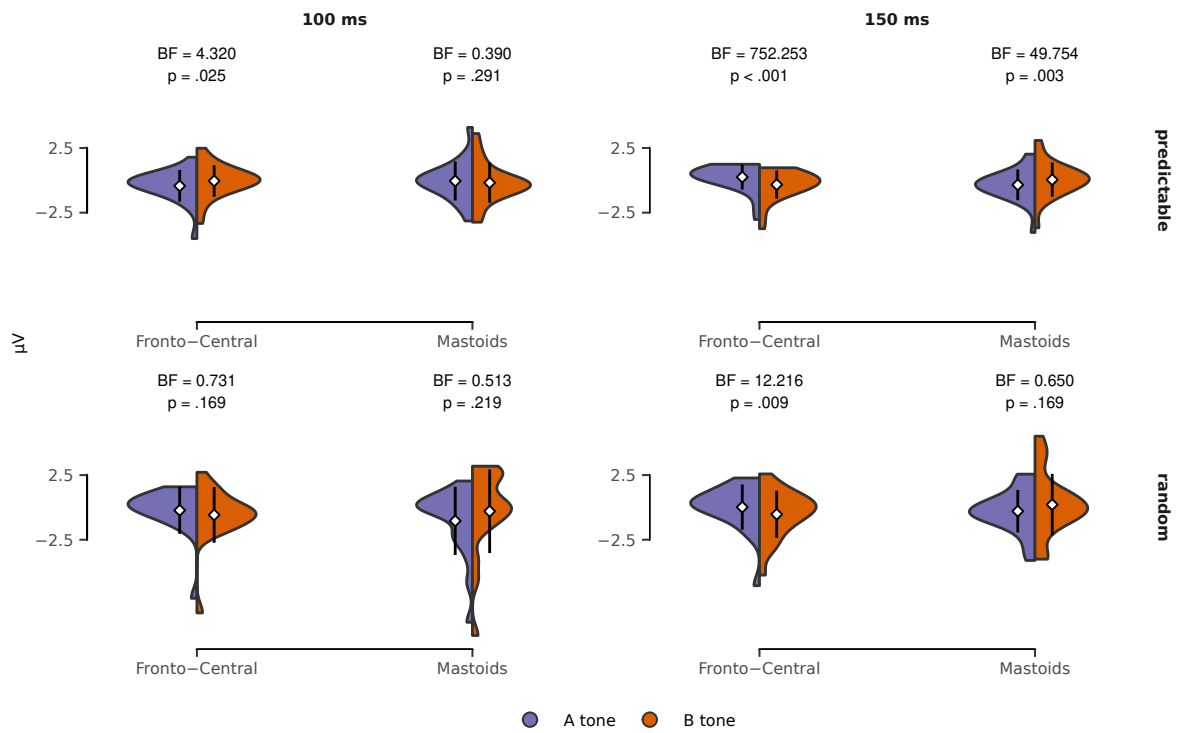
Post-hoc tests between ERPs to A and B tones were carried out using two-tailed Student's *t*-tests complementary Bayesian analysis. P-values were corrected for multiple comparisons using the Benjamini–Hochberg step-up procedure. For the 100 ms SOA, results indicated a significant effect only for predictable tones at fronto-central electrodes ($t(19) = -2.77, 0.0246, CI_{.95} = [-0.67, -0.09]$). For the 150 ms SOA, B tones elicited significantly more negative ERPs than A tones at fronto-central electrode locations in both predictable ($t(22) = 5.20, 0.0002584, CI_{.95} = [0.35, 0.81]$) and random ($t(22) = 3.28, 0.009093333333333333, CI_{.95} = [0.20, 0.91]$) conditions. Significant polarity reversal effects at mastoid sites were only present for predictable ($t(22) = -3.95, 0.002716, CI_{.95} = [-0.61, -0.19]$) tones but not for randomly presented ($t(22) = -1.59, 0.1693333333333333, CI_{.95} = [-1.18, 0.16]$) tones.

To investigate whether absence of evidence for an MMN might be due to low within-participant sample sizes, the analysis was repeated for the *random* condition including not only B tone trials that occurred within a five-tone sequence (as with the pre-registered analysis path), but all B tones and their immediately preceding A tone. Results from this comparison are shown in (Fig?):??.

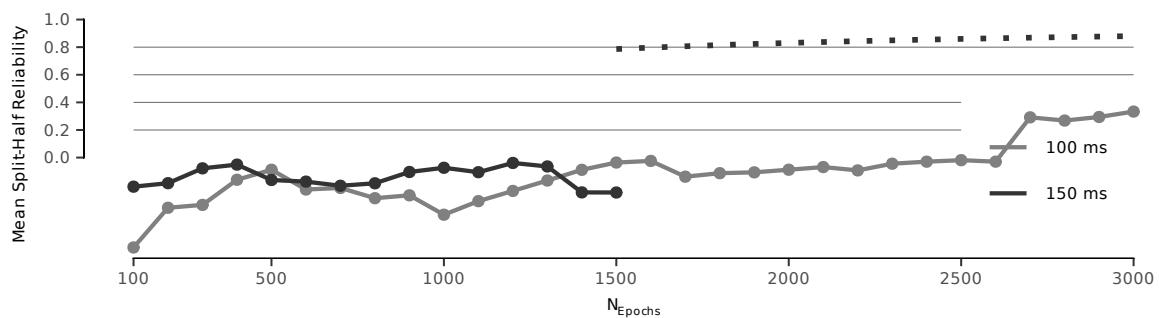
Split-half reliabilities are displayed in fig. 5. Simulated values match the curve expected from the Spearman-Brown formula. In the context of classical test theory, this method relates the length of a test (or *experiment*) to the number of items (or *trials*). The first derivative of the Spearman-Brown function is monotonically decreasing, leading to two different observations: i) Adding additional epochs (extending the test length by an absolute value in classical test theory terms) has a large effect when the number of already present epochs is low, but has only little

Figure 4.

Averaged voltages in the MMN latency window for pooled fronto-central and mastoid electrodes. Colored areas show sample probability density function for A tones (green) and B tones (red). White diamonds indicate estimated population mean, vertical bars represent 95%-confidence interval. Only Benjamini-Hochberg-corrected p -values < 0.05 are shown.

**Figure 5.**

EEG waveforms for five-tone sequences presented in an predictable context (dotted line) and pseudo-random condition (dashed line) for 100 ms presentation rate (top panel) and 150 ms presentation rate (lower panel). Vertical lines indicate tone onset.



effect when already dealing with large numbers of epochs and ii) SOA and thus effect sized have a larger impact when epoch numbers are small compared to high epoch numbers. Graphed values also show that reliabilities for the 100 ms stimulation rate are considerably lower than for an SOA of 150 ms and that reliabilities are very low when using a relatively small number of epochs. There is no generally accepted rule as to the level above which the coefficient can be considered acceptable. Rather, reliability should be evaluated based on the purpose of a study considering the cost-benefit trade-off (Nunnally et al., 1994). As laid out, increased reliability comes at overproportionate cost, in that collecting more samples will not increase reliability by the same factor. That said, many published articles deem reliability coefficients above .7 or .8 “acceptable” (Lance et al., 2006).

Table 2

Results of the 3-way ANOVA (condition x stimulus x electrode) for repeated measures conducted on the mean ERP-amplitudes (time window 111 - 161 ms) at electrode Fz (upper section). The significant interaction between the three factors included was further analyzed by 2-way ANOVAS (stimulus x electrode) conducted separately for the random condition (middle section) and the predictable condition (lower section).

	Effect	DFn	DFd	F	p	p<.05	ges
100 ms	Condition	1	19	0.831	0.373		0.008
	StimulusType	1	19	1.05	0.318		0.002
	Electrode	1	19	0.036	0.852		0.000331
	Condition x StimulusType	1	19	0.051	0.823		7.55e-05
	Condition x Electrode	1	19	0.763	0.393		0.002
	StimulusType x Electrode	1	19	0.797	0.383		0.001
	Condition x StimulusType x Electrode	1	19	7.53	0.013	*	0.01
150 ms	Condition	1	22	0.08	0.78		0.000263
	StimulusType	1	22	0.317	0.579		0.000339
	Electrode	1	22	0.035	0.854		0.000301
	Condition x StimulusType	1	22	0.16	0.693		0.000124
	Condition x Electrode	1	22	1.13	0.299		0.003
	StimulusType x Electrode	1	22	20.8	0.000155	*	0.026
	Condition x StimulusType x Electrode	1	22	0.053	0.819		4.63e-05

Table 3

Results of the 3-way ANOVA (condition x stimulus x electrode) for repeated measures conducted on the mean ERP-amplitudes (time window 111 - 161 ms) at electrode Fz (upper section). The significant interaction between the three factors included was further analyzed by 2-way ANOVAS (stimulus x electrode) conducted separately for the random condition (middle section) and the predictable condition (lower section).

		Effect	DFn	DFd	F	p	p<.05	ges
100 ms	Frontal	Condition	1	19	0.16	.694		0.003
		StimulusType	1	19	0.006	.938		1.5e-05
		Condition x StimulusType	1	19	16.7	< .001	*	0.013
	Mastoids	Condition	1	19	1.28	.272		0.014
		StimulusType	1	19	1.21	.285		0.004
		Condition x StimulusType	1	19	2.37	.141		0.009
150 ms	Frontal	Condition	1	22	0.947	.341		0.006
		StimulusType	1	22	22.7	< .001	*	0.038
		Condition x StimulusType	1	22	0.028	.868		2.2e-05
	Mastoids	Condition	1	22	0.206	.655		0.001
		StimulusType	1	22	6.56	.018	*	0.018
		Condition x StimulusType	1	22	0.122	.730		0.00028

Discussion

We did not replicate

For the 150 presentation, extreme evidence for an MMN and very strong evidence for an accopying polarity reversal at the mastoids was found in the *predictable* condition, that is, when tones were presented in an repeated five-tone pattern. When tones were presented in random order, strong evidence was found for an MMN but Bayes factors suggested inconclusive evidence for mastoids. In light of the resuts by E. S. Sussman & Gumenyuk (2005), we would

Lorem ipsum dolor sit amet, consectetur adipiscing elit. Donec id cursus velit, non egestas quam. Aliquam rutrum eget sem ut aliquet. Etiam euismod purus et gravida volutpat. Suspendisse consequat ipsum nibh, vitae convallis dolor efficitur a. Suspendisse vehicula erat posuere velit fermentum viverra. Proin sapien urna, iaculis ut ultricies ac, auctor eu est. Nunc ornare pharetra finibus. Morbi finibus, ipsum non accumsan cursus, metus nisl egestas leo, et aliquam nisi leo quis diam. Quisque id diam non risus elementum convallis. Duis non nisl at nisl imperdiet vestibulum. Suspendisse efficitur porttitor nulla a vehicula. Interdum et malesuada fames ac ante ipsum primis in faucibus. Praesent tempor urna in orci congue, non euismod eros volutpat. Integer ullamcorper auctor libero, in laoreet nulla hendrerit ultrices.

Proin malesuada nisi et luctus volutpat. Nam ac posuere enim. Proin nec augue tincidunt felis ullamcorper luctus ac sit amet mi. Maecenas aliquam leo quis enim gravida maximus. Sed nec pellentesque magna. Vivamus et purus lacus. Donec maximus purus at fermentum efficitur. Phasellus auctor orci sem, eu sollicitudin eros pretium a.

In maximus libero at purus lobortis efficitur. Aliquam nec sapien consequat, lobortis lorem id, luctus velit. Pellentesque habitant morbi tristique senectus et netus et malesuada fames ac turpis egestas. Vestibulum dictum ipsum eu nunc maximus, quis ornare augue tincidunt. Nam leo purus, mollis quis nunc sed, sagittis tempus orci. In condimentum et neque ut laoreet. Curabitur accumsan ligula eu libero iaculis ullamcorper. Interdum et malesuada fames ac ante ipsum primis in faucibus. Nullam iaculis tellus risus, vitae dapibus augue commodo a. Sed ante dolor, fermentum at lectus id, pulvinar viverra elit. Aenean tincidunt mollis imperdiet.

Nulla id molestie neque, vitae vulputate velit. Fusce a velit imperdiet felis porttitor
 scelerisque. Nam tempus tincidunt elit, id finibus tortor tristique non. Ut imperdiet finibus
 mauris, in fringilla mauris blandit auctor. Etiam volutpat quam et feugiat elementum. Duis
 finibus fermentum condimentum. Donec sollicitudin molestie dolor. Cras convallis lorem orci,
 ut sagittis risus rutrum eget. Donec vel lobortis justo.

Pellentesque habitant morbi tristique senectus et netus et malesuada fames ac turpis
 egestas. Proin non leo vehicula, congue elit faucibus, tincidunt diam. Sed euismod vulputate
 mauris. Duis dapibus faucibus arcu, ut vehicula tellus blandit eu. Duis erat magna, cursus quis
 urna nec, placerat blandit lectus. Maecenas dolor quam, pharetra a urna eu, mollis iaculis dolor.
 Aliquam maximus ante eget felis faucibus porta. Cras semper felis non tellus rutrum tempus.
 Morbi quam metus, volutpat nec aliquam at, interdum a nibh. Sed hendrerit purus tempor ex
 placerat, ut fringilla nulla molestie. Nullam vitae sem non purus lobortis fermentum. Quisque
 ligula tellus, ullamcorper sit amet consectetur quis, fermentum ac mi. Nunc pretium mollis
 dictum. # References

Ablin, P., Cardoso, J.-F., & Gramfort, A. (2018). Faster independent component analysis by
 preconditioning with Hessian approximations. *IEEE Transactions on Signal Processing*, 66(15),
 4040–4049. <https://doi.org/10.1109/TSP.2018.2844203>

Ablin, P., Cardoso, J.-F., & Gramfort, A. (2017). Faster ICA under orthogonal constraint.
arXiv:1711.10873 [Stat]. <http://arxiv.org/abs/1711.10873>

Aczel, B., Palfi, B., Szollosi, A., Kovacs, M., Szaszi, B., Szecsi, P., Zrubka, M., Gronau, Q. F., Bergh,
 D. van den, & Wagenmakers, E.-J. (2018). Quantifying Support for the Null Hypothesis in
 Psychology: An Empirical Investigation: *Advances in Methods and Practices in Psychological
 Science*. <https://doi.org/10.1177/2515245918773742>

Alain, C., Woods, D. L., & Ogawa, K. H. (1994). Brain indices of automatic pattern processing:
NeuroReport, 6(1), 140–144. <https://doi.org/10.1097/00001756-199412300-00036>

Bigdely-Shamlo, N., Mullen, T., Kothe, C., Su, K.-M., & Robbins, K. A. (2015). The PREP pipeline:

standardized preprocessing for large-scale EEG analysis. *Frontiers in Neuroinformatics*, 9.
<https://doi.org/10.3389/fninf.2015.00016>

Brainard, D. H. (1997). The Psychophysics Toolbox. *Spatial Vision*, 10(4), 433–436.
<https://doi.org/10.1163/156856897X00357>

Brown, W. (1910). SOME EXPERIMENTAL RESULTS IN THE CORRELATION OF MENTAL
ABILITIES1. *British Journal of Psychology*, 1904-1920, 3(3), 296–322.
<https://doi.org/10.1111/j.2044-8295.1910.tb00207.x>

Carpenter, B., Gelman, A., Hoffman, M. D., Lee, D., Goodrich, B., Betancourt, M., Brubaker, M.,
Guo, J., Li, P., & Riddell, A. (2017). Stan: A Probabilistic Programming Language. *Journal of
Statistical Software*, 76(1), 1–32. <https://doi.org/10.18637/jss.v076.i01>

de Cheveigné, A. (2020). ZapLine: A simple and effective method to remove power line artifacts.
NeuroImage, 207, 116356. <https://doi.org/10.1016/j.neuroimage.2019.116356>

de Cheveigné, A., & Nelken, I. (2019). Filters: When, Why, and How (Not) to Use Them. *Neuron*,
102(2), 280–293. <https://doi.org/10.1016/j.neuron.2019.02.039>

Delorme, A., & Makeig, S. (2004). EEGLAB: an open source toolbox for analysis of single-trial
EEG dynamics including independent component analysis. *Journal of Neuroscience Methods*,
134(1), 9–21. <https://doi.org/10.1016/j.jneumeth.2003.10.009>

Goodman, S. (2008). A Dirty Dozen: Twelve P-Value Misconceptions. *Seminars in Hematology*,
45(3), 135–140. <https://doi.org/10.1053/j.seminhematol.2008.04.003>

Gramfort, A. (2013). MEG and EEG data analysis with MNE-Python. *Frontiers in Neuroscience*, 7.
<https://doi.org/10.3389/fnins.2013.00267>

Hubbard, R. (2011). The widespread misinterpretation of p-values as error probabilities. *Journal
of Applied Statistics*, 38(11), 2617–2626. <https://doi.org/10.1080/02664763.2011.567245>

Hubbard, R., & Lindsay, R. M. (2008). Why P Values Are Not a Useful Measure of Evidence in

461 Statistical Significance Testing: *Theory & Psychology*.

462 <https://doi.org/10.1177/0959354307086923>

463 Kirk, R. E. (1996). Practical Significance: A Concept Whose Time Has Come. *Educational and*

464 *Psychological Measurement*, 56(5), 746–759. <https://doi.org/10.1177/0013164496056005002>

465 Kleiner, M., Brainard, D., Pelli, D., Ingling, A., Murray, R., & Broussard, C. (2007). What's new in
466 psychtoolbox-3. *Perception*, 36(14), 1–16.

467 <https://nyuscholars.nyu.edu/en/publications/whats-new-in-psychtoolbox-3>

468 Lance, C. E., Butts, M. M., & Michels, L. C. (2006). The Sources of Four Commonly Reported

469 Cutoff Criteria: What Did They Really Say? *Organizational Research Methods*, 9(2), 202–220.

470 <https://doi.org/10.1177/1094428105284919>

471 Meehl, P. E. (1978). Theoretical risks and tabular asterisks: Sir Karl, Sir Ronald, and the slow
472 progress of soft psychology. *Journal of Consulting and Clinical Psychology*, 46(4), 806–834.

473 <https://doi.org/10.1037/0022-006X.46.4.806>

474 Mullen, T. R., Kothe, C. A. E., Chi, Y. M., Ojeda, A., Kerth, T., Makeig, S., Jung, T.-P., &

475 Cauwenberghs, G. (2015). Real-time neuroimaging and cognitive monitoring using wearable
476 dry EEG. *IEEE Transactions on Biomedical Engineering*, 62(11), 2553–2567.

477 <https://doi.org/10.1109/TBME.2015.2481482>

478 Nordby, H., Roth, W. T., & Pfefferbaum, A. (1988). Event-Related Potentials to Breaks in

479 Sequences of Alternating Pitches or Interstimulus Intervals. *Psychophysiology*, 25(3), 262–268.

480 <https://doi.org/10.1111/j.1469-8986.1988.tb01239.x>

481 Nunnally, J., Jum, N., Bernstein, I. H., & Bernstein, I. (1994). *Psychometric Theory*. McGraw-Hill

482 Companies, Incorporated.

483 Oldfield, R. C. (1971). The assessment and analysis of handedness: the Edinburgh inventory.

484 *Neuropsychologia*, 9(1), 97–113. [https://doi.org/10.1016/0028-3932\(71\)90067-4](https://doi.org/10.1016/0028-3932(71)90067-4)

485 Paavilainen, P. (2013). The mismatch-negativity (MMN) component of the auditory

event-related potential to violations of abstract regularities: A review. *International Journal of Psychophysiology*, 88(2), 109–123. <https://doi.org/10.1016/j.ijpsycho.2013.03.015>

Perrin, F., Pernier, J., Bertrand, O., & Echallier, J. F. (1989). Spherical splines for scalp potential and current density mapping. *Electroencephalography and Clinical Neurophysiology*, 72(2), 184–187. [https://doi.org/10.1016/0013-4694\(89\)90180-6](https://doi.org/10.1016/0013-4694(89)90180-6)

Pion-Tonachini, L., Kreutz-Delgado, K., & Makeig, S. (2019). ICLabel: An automated electroencephalographic independent component classifier, dataset, and website. *NeuroImage*, 198, 181–197. <https://doi.org/10.1016/j.neuroimage.2019.05.026>

Popper, K. (1935). *Logik der Forschung: Zur Erkenntnistheorie der Modernen Naturwissenschaft*. Springer Vienna.

Rouder, J. N., Speckman, P. L., Sun, D., Morey, R. D., & Iverson, G. (2009). Bayesian t tests for accepting and rejecting the null hypothesis. *Psychonomic Bulletin & Review*, 16(2), 225–237. <https://doi.org/10.3758/PBR.16.2.225>

Saarinen, J., Paavilainen, P., Schöger, E., Tervaniemi, M., & Näätänen, R. (1992). Representation of abstract attributes of auditory stimuli in the human brain: *NeuroReport*, 3(12), 1149–1151. <https://doi.org/10.1097/00001756-199212000-00030>

Scharf, F., & Müller, D. (in prep). *Predictable changes within fast-paced sound sequences do not elicit the mismatch negativity: An in-class replication study*.

Schmidt, S. (2009). Shall we Really do it Again? The Powerful Concept of Replication is Neglected in the Social Sciences: *Review of General Psychology*. <https://doi.org/10.1037/a0015108>

Schröger, E., Tervaniemi, M., Wolff, C., & Näätänen, R. N. (1996). Preattentive periodicity detection in auditory patterns as governed by time and intensity information. *Cognitive Brain Research*, 4(2), 145–148. [https://doi.org/10.1016/0926-6410\(96\)00023-7](https://doi.org/10.1016/0926-6410(96)00023-7)

Sellke, T., Bayarri, M. J., & Berger, J. O. (2001). Calibration of p Values for Testing Precise Null Hypotheses. *The American Statistician*, 55(1), 62–71.

<https://doi.org/10.1198/000313001300339950>

Spearman, C. (1910). Correlation calculated from faulty data. *British Journal of Psychology*, 3, 271–295.

Stan Development Team. (2020). *RStan: the R interface to Stan*. <http://mc-stan.org/>

Sussman, E., Ritter, W., & Vaughan, H. G. (1998). Predictability of stimulus deviance and the mismatch negativity: *NeuroReport*, 9(18), 4167–4170.

<https://doi.org/10.1097/00001756-199812210-00031>

Sussman, E. S., & Gumenyuk, V. (2005). Organization of sequential sounds in auditory memory: *NeuroReport*, 16(13), 1519–1523. <https://doi.org/10.1097/01.wnr.0000177002.35193.4c>

Wagenmakers, E.-J. (2007). A practical solution to the pervasive problems of p values.

Psychonomic Bulletin & Review, 14(5), 779–804. <https://doi.org/10.3758/BF03194105>

Wagenmakers, E.-J., Marsman, M., Jamil, T., Ly, A., Verhagen, J., Love, J., Selker, R., Gronau, Q. F., Šmíra, M., Epskamp, S., Matzke, D., Rouder, J. N., & Morey, R. D. (2018). Bayesian inference for psychology. Part I: Theoretical advantages and practical ramifications. *Psychonomic Bulletin & Review*, 25(1), 35–57. <https://doi.org/10.3758/s13423-017-1343-3>

Widmann, A., Schröger, E., & Maess, B. (2015). Digital filter design for electrophysiological data – a practical approach. *Journal of Neuroscience Methods*, 250, 34–46.

<https://doi.org/10.1016/j.jneumeth.2014.08.002>

Winkler, I., Debener, S., Müller, K.-R., & Tangermann, M. (2015). On the influence of high-pass filtering on ICA-based artifact reduction in EEG-ERP. *2015 37th Annual International Conference of the IEEE Engineering in Medicine and Biology Society (EMBC)*, 4101–4105.

<https://doi.org/10.1109/EMBC.2015.7319296>